



## Validation of static and dynamic radiostereometric analysis of the knee joint using bone-models from CT data

Stentz-Olesen, Kasper; Nielsen, Emil Toft; de Raedt, Sepp; Jørgensen, Peter Bo; Sørensen, Ole Gade; Kaptein, Bart; Andersen, Michael Skipper; Stilling, Maiken

*Published in:*  
Bone & Joint Research

*DOI (link to publication from Publisher):*  
[10.1302/2046-3758.66.BJR-2016-0113.R3](https://doi.org/10.1302/2046-3758.66.BJR-2016-0113.R3)

*Publication date:*  
2017

*Document Version*  
Accepted author manuscript, peer reviewed version

[Link to publication from Aalborg University](#)

*Citation for published version (APA):*  
Stentz-Olesen, K., Nielsen, E. T., de Raedt, S., Jørgensen, P. B., Sørensen, O. G., Kaptein, B., Andersen, M. S., & Stilling, M. (2017). Validation of static and dynamic radiostereometric analysis of the knee joint using bone-models from CT data. *Bone & Joint Research*, 6(6), 376-384. <https://doi.org/10.1302/2046-3758.66.BJR-2016-0113.R3>

### General rights

Copyright and moral rights for the publications made accessible in the public portal are retained by the authors and/or other copyright owners and it is a condition of accessing publications that users recognise and abide by the legal requirements associated with these rights.

- Users may download and print one copy of any publication from the public portal for the purpose of private study or research.
- You may not further distribute the material or use it for any profit-making activity or commercial gain
- You may freely distribute the URL identifying the publication in the public portal -

### Take down policy

If you believe that this document breaches copyright please contact us at [vbn@aub.aau.dk](mailto:vbn@aub.aau.dk) providing details, and we will remove access to the work immediately and investigate your claim.

1 **Title page**

2  
3 **Validation of static and dynamic radiostereometric analysis of the**  
4 **knee joint using bone-models from CT data.**

5  
6 K Stentz-Olesen<sup>1</sup>, ET Nielsen<sup>1</sup>, S De Raedt<sup>2</sup>, PB Jørgensen<sup>1</sup>, OG Sørensen<sup>1</sup>,  
7 BL Kaptein<sup>3</sup>, MS Andersen<sup>4</sup>, M Stilling<sup>1,5</sup>

8  
9  
10 *1: Orthopedic Research Group, Department of Orthopedic Surgery, Aarhus University Hospital,*  
11 *Denmark*

12 *2: Research and Development, Nordisk Røntgen Teknik, Denmark.*

13 *3: Biomechanics and Imaging Group, Department of Orthopedic Surgery, LUMC, The Netherlands*

14 *4: Department of Mechanical Engineering and Manufacturing, Aalborg University, Denmark*

15 *5: Department of Clinical Medicine, University of Aarhus, Denmark*

16  
17 Submitting for Original Article

18  
19 **CORRESPONDING AUTHOR:**

20 Kasper Stentz-Olesen  
21 Orthopedic Research Group, Department of Orthopedic Surgery,  
22 Aarhus University Hospital, Denmark  
23 Tage-Hansens Gade 2, building 10A, office 13, 8000 Aarhus C.  
24 kasperstentz@gmail.com  
25 Phone +45 28696688

26  
27  
28  
29  
30  
31  
32  
33  
34

## Author's Contributions

- 35
- 36
- 37 Title: Validation of static and dynamic radiostereometric analysis of the knee joint using bone-models from CT data.
- 38 Article Type: Original Article
- 39 MSc Kasper Stentz-Olesen: kasperstentz@gmail.com  
40 Orthopaedic Research Unit, Aarhus University Hospital, Tage Hansens Gade 2, 8000 Aarhus C, Denmark  
41 Substantial contribution to the research design, acquisition of data, analysis and interpretation of data. Writing the  
42 first draft of the paper.  
43
- 44 MSc, PhD student Emil Toft Nielsen: emil.toft@gmail.com  
45 Department of Health Science and Technology, Aalborg University, Fredrik Bajers Vej 7 D2, 9220 Aalborg East,  
46 Denmark  
47 Orthopaedic Research Unit, Aarhus University Hospital, Tage Hansens Gade 2, 8000 Aarhus C, Denmark  
48 Substantial contribution to the research design, acquisition, analysis and interpretation of data, and revising the  
49 paper critically.  
50
- 51 MSc, PhD Sepp De Raedt: sepp.de.raedt@clin.au.dk  
52 Nordisk Røntgen Teknik, Birkegårdsvej 16, 8361 Hesselager, Denmark  
53 Substantial contributions to research design, analysis of data, interpretation of data and revising the paper critically.  
54
- 55 MSc, PhD student Peter Bo Jørgensen: pbjr@clin.au.dk  
56 Orthopaedic Research Unit, Aarhus University Hospital, Tage Hansens Gade 2, 8000 Aarhus C, Denmark  
57 Substantial contribution to the research design, acquisition of data and revising the paper critically.  
58
- 59 MD, PhD Ole Gade Sørensen: ole.gade.soerensen@vest.rm.dk  
60 Orthopaedic Research Unit, Aarhus University Hospital, Tage Hansens Gade 2, 8000 Aarhus C, Denmark  
61 Substantial contribution to the research design, acquisition of data and revising the paper critically.  
62
- 63 MSc, PhD Bart Kaptein: B.L.Kaptein@lumc.nl  
64 Biomechanics and Imaging Group, Department of Orthopedic Surgery, Leiden University Medical Center,  
65 Albinusdreef 2, 2333 ZA Leiden, Netherlands  
66 B.L.Kaptein@lumc.nl  
67 Substantial contributions to analysis and interpretation of data and revising the paper critically.  
68
- 69 MSc, PhD, Associate Professor Michael Skipper Andersen: msa@m-tech.aau.dk  
70 Department of Mechanical Engineering and Manufacturing, Aalborg University, Denmark, Fibigerstræde 16, 9220  
71 Aalborg East, Denmark  
72 Substantial contributions to analysis and interpretation of data and revising the paper critically.  
73
- 74 MD, PhD, Associate Professor Maiken Stilling: maiken.stilling@clin.au.dk  
75 Orthopedic Research Group, Department of Orthopedic Surgery, Aarhus University Hospital, Denmark  
76 Department of Clinical Medicine, University of Aarhus, Denmark  
77 Substantial contribution to the research design acquisition of data, interpretation of data and revising the paper  
78 critically.  
79
- 80 All authors have read, commented and approved the final submitted manuscript.  
81
- 82
- 83

84 **ABSTRACT**

85 Objectives: Static radiostereographic analysis (RSA) using implanted markers are considered the most  
86 accurate system for the evaluation of prosthesis migration. By using computed tomography bone-models  
87 instead of markers combined with a dynamic RSA system, a non-invasive measurement of joint motion is  
88 enabled. This method is more accurate than current 3D skin marker-based tracking systems. The purpose  
89 of this study was to evaluate the accuracy of the CT model-method for measuring knee joint kinematics in  
90 static and dynamic RSA using the marker-method as the gold standard.

91 Methods: Bone-models were created from CT scans, and tantalum beads were implanted into the tibia and  
92 femur of eight human donor knees. Each specimen was secured in a fixture, static and dynamic stereo  
93 radiographs were recorded, and the bone-models and the marker-models were fitted to the stereo  
94 radiographs.

95 Results: Results showed a mean difference between the two methods in all six degrees of freedom  
96 (6DOF) for static RSA to be within  $-0.10$  to  $0.08$  mm/ $^{\circ}$  with a 95% Limit of Agreement (LoA) ranging  
97 from  $\pm 0.49 - 1.26$ . Dynamic RSA had a slightly larger range in mean difference of  $-0.23 - 0.16$  mm/ $^{\circ}$   
98 with LoA ranging from  $\pm 0.75 - 1.50$ .

99 Conclusions: In a laboratory controlled setting, the CT model method combined with dynamic RSA may  
100 be an alternative to prior marker-based methods for kinematic analyses.

101 **KEYWORDS:**

102 Radiostereographic analysis, Dynamic, CT bone-model

103

104

105

106

107

108

109

110 **Article focus:**

- 111 • Validation of the accuracy of a model-method using CT bone-models for measuring knee joint  
112 kinematics in static and dynamic radiostereometric analysis using the marker-method as the gold  
113 standard.

114  
115 **Key messages:**

- 116 • We believe the accuracy of the CT model-method combined with static and dynamic  
117 radiostereometry is sufficient when examining large joints. However, for the method to be truly  
118 effective, an automated analysis method should be developed.
- 119 • The CT model-method could be the favorable method in future kinematic studies of large joints,  
120 since no implanted markers are needed.
- 121

122 **Strengths and limitations of this study:**

123 Eight donor legs were used for this study, and potentially the small sample size may lead to an  
124 overestimation of the accuracy.

- 125 • The following processes were automated, and the reproducibility of the processes was therefore  
126 not investigated.
- 127 • CT-segmentation of the bone model.
  - 128 • Placing the anatomical coordinate system.
  - 129 • Detection and creation of the markers model.
- 130 •
- 131 • The comparison of the model-method and the marker-method was not blinded.

132 **1.INTRODUCTION**

133

134 To perform kinematic analysis of joints, an accurate and reliable method of tracking bone motion is  
135 needed (1). In radiostereometric analysis (RSA), tantalum markers are inserted into the bone during  
136 surgery to track the bones with stereo x-rays. This is currently widely used to monitor implant fixation  
137 and wear over time (2–4). RSA measurements have been shown to be very accurate and precise at the  
138 submillimeter level (2,5,6).

139 Dual-plane fluoroscopy using computed tomography (CT) bone-models have been used to record and  
140 calculate knee joint kinematics without markers (7–9). In 2003, a model-based RSA method was  
141 introduced allowing prosthesis tracking without the use of markers at the expense of a slight accuracy loss  
142 (10,11).

143 The accuracy of dynamic RSA using CT bone-models is expected to be similar to dynamic RSA using  
144 models of prostheses, which would be acceptable in studies examining movements of large joints. The

145 CT-bone-model-RSA method would be superior to skin marker based joint kinematics measurements that  
146 are exposed to soft tissue artefacts (1,12,13). Further, the model-method enables kinematic and stability  
147 comparison between pre-operative and post-operative, and injured and healthy joints without the need of  
148 inserting bone markers.

149 The purpose of this study was to evaluate the accuracy of the CT model-method for measuring knee joint  
150 kinematics with static and dynamic RSA using the marker-method as the gold standard.

## 151 2.MATERIAL AND METHODS

### 152 *2.1 Specimens and dissection*

153 Eight paired fresh-frozen human (four female, four male) donor legs including foot, knee and hemipelvis  
154 were used for this study. Two of the donor knees had degenerative changes. The mean age of the  
155 specimens was 77 years.

### 156 *2.2 Preparations for the RSA analysis*

157 A bead-insertion instrument (Kulkanon, Wennbergs Finmek, Sweden) was used to place eight to twelve 1  
158 mm tantalum beads widely spread in the cortical bone of femur and tibia approximately five cm from the  
159 joint line through a 4 mm drill hole on the lateral side of the proximal tibia and the medial side of the  
160 distal femur.

### 161 *2.3 CT bone-model*

162 The intact frozen leg specimens were scanned in a Phillips Brilliance 40 CT scanner using axial slices,  
163 120 kVp, 150 mAs, slice thickness = 0.9mm, slice increment = 0.45mm, pixel size = 0.39mm×0.39mm.

164 The bone-models were constructed using an automatic graph-cut segmentation method (14,15). The  
165 method uses eigen analysis of the hessian matrix to identify the sheet-like structure of the bone surface  
166 and formulate a sheetness measure, which is subsequently used in a graph-cut optimization (16).

167 The reconstructed bone-models (figure a) included approximately 15cm of both the distal femur and  
168 proximal tibia. For each bone-model, a local coordinate system was created using a modified version of

169 the automatic method introduced by Miranda et al. (2010), where the diaphysis was fitted using a cylinder  
170 instead of the principal component analysis used by Miranda.

#### 171 ***2.4 Experimental setup and equipment:***

172 A custom build motorized fixture was built to support the thigh and lower leg while the area of the knee  
173 was kept completely free of materials to avoid image artefacts. The hemipelvis was fixed to the base of  
174 the apparatus using three regular screws in the sacrum, iliac crest and the pubic bone. The foot and ankle  
175 joint were fixed in a standard PRO+ FIXED WALKER (VQ OrthoCare, Irvine, USA). A stepper motor  
176 (NEMA 23, 3Nm, National Instruments) was installed along with pulley wheels, a timing belt and two  
177 linear slides to perform the controlled dynamic knee flexion motion from 0° to 60° of flexion and back at  
178 0.1m/s. The recorded knee flexion angles were limited to be from 0° to 60° due to limitations in the size  
179 of the systems region of interest. Another NEMA 23 motor was mounted to the foot rest – making the  
180 internal rotation of the foot automatic at a speed of 0.001m/s. The slow speed enabled a manual stop of  
181 the motor when the desired torque was reached. The torque was measured using a torque sensor (TQ 201-  
182 500, OMEGA, USA) (accuracy = ±0.15%, repeatability = ±0.03%) and an adjacent meter (DP25B-S-230,  
183 OMEGA, USA). Both motors were controlled using a driver (DM542A, Longs Motor, China) and a  
184 breakout board (DB25, Sunwin, China). Figure b shows the set-up.

#### 185 ***2.5 Radiographic setup***

186 The stereo radiographs were recorded using a dynamic RSA system (Adora RSAd, Nordisk Røntgen  
187 Teknik, Denmark). A sampling frequency of 10 frames/sec, a vertically placed calibration box with  
188 uniplanar detectors (Box 14; Medis Specials, Leiden, the Netherlands) and a vertical tube set-up (±16  
189 degrees tube angle to horizontal) were used to maximize the visualization of the knee joint line during  
190 motion. The full detector size of 37 (horizontal) x 42cm was utilized for each detector to record the knee  
191 motion from 0° to 60° of knee flexion. The source image distance (SID) was 2.94m and the focus skin  
192 distance (FSD) was 2.4m, and were chosen to increase the region of interest. The exposure settings for  
193 static radiographs were; 70KV and 10mAs. For the dynamic radiographs it was; 90KV, 500mA, 2.5ms

194 roentgen pulse width and a synchronization delay between tubes of approx. 0.002ms (maximum allowed  
195 by the system = 0.1ms). The resolution of the static radiographs was 2208x 2688 pixels (0.16mm/pixel)  
196 and for the dynamic radiographs it was 1104x1344 pixels (0.32mm/pixel). The difference in resolution is  
197 due to limitations of the RSA system.

## 198 ***2.6 Test protocol***

199 Step 1; static stereo radiographs were recorded with the donor legs positioned in 0°, 30° and 60° of knee  
200 flexion measured with a goniometer. 4Nm of internal rotation torque was applied to the foot to simulate a  
201 loaded knee before recording. Step 2; dynamic RSA series (10 frames/sec) were recorded in two  
202 successive runs of motorized driven knee motion (~0.08 m/s) from 0° to 60° of knee flexion. 4Nm of  
203 internal rotatory torque was applied to the foot before recording, and the reached internal rotation angle  
204 was kept throughout the sequence, meaning that the applied internal torque varied during the recording.  
205 Step 3; the leg was repositioned, and step 1 and 2 was repeated. The specimens were simultaneously used  
206 in another study that assessed ligament stability in five situations, where the anterior cruciate ligament  
207 (ACL) and the anterolateral ligament (ALL) were successively cut and reconstructed and compared with  
208 the intact knee. A total of eight (legs) x three (flexion angles) x two (double examinations) x five  
209 (ligament situations) = 240 static radiographs were recorded.

210 From the dynamic series, radiographs were selected so they matched the static radiographs with knee  
211 flexion angles of 0°, 30° and 60° as determined by model position of tibia and femur during radiographic  
212 image analysis in ModelBasedRSA (MBRSA) and two ligament situations were used, resulting in eight x  
213 three x two x two = 96 dynamic radiographs.

## 214 ***2.7 Analysis of the radiographs***

215 Of the 240 planned static and 96 dynamic stereo radiographs, 228 static and 89 dynamic radiographs were  
216 used. Six static and three dynamic trials were not recorded by mistake, and in six static images and four  
217 dynamic trials, the fixture was positioned incorrectly. Of the 228 static radiographs, 139 (~ 3/5 of the  
218 240 minus exclusions) were used to obtain a good alignment between the local coordinate systems of the

219 model-method and the marker-method. The remaining 2/5 ~ 89 (minus exclusions) static and dynamic  
220 radiographs were used to calculate the difference between the model-method and the marker-method.  
221 The static and dynamic radiographs were analyzed using the commercially available software; Model-  
222 Based RSA v.4.02 , RSAcore, Leiden. MBRSA automatically detects the bone contours and an operator  
223 needs to select the contours to be included in the pose estimation algorithm. The selected contours (figure  
224 c) for the femur were the shaft, the condyles and the articular surface, while for the tibia the shaft, the  
225 eminencies and the medial and lateral plateau were selected. The process of fitting the bone-models to the  
226 radiographs was done by two observers, who previously in a pilot study fitted 25 femur and tibia bone-  
227 models and together developed a consistent workflow to ensure that the same contours were used as much  
228 as possible.

229 The MBRSA software's three algorithms (17) were applied and used to estimate the pose of each CT-  
230 model by minimizing the matching error between the virtual projection of the bone-model and the  
231 detected projection (contours) in the radiograph.

232 The mean error of rigid body fitting is used to assess the mean error of marker detection between frames  
233 within a rigid body, and is recommended to be below 0.35mm (18). The mean condition number is used  
234 to assure an acceptable scatter of the injected markers, and is recommended to be below 120 in studies of  
235 the knee (18,19). The average mean error and the condition number for femur and tibia were calculated in  
236 89 static and 89 dynamic radiographs.

### 237 ***2.8 Inter- and intra-observer reliability measurements of the manual contour selection***

238 Inter- and intra-reliability measurements were performed of the manual contour selection and were  
239 completed by three observers. The observers (Obs.) were categorized as experienced (Obs. 1 with +500  
240 RSA analysis), less experienced (Obs. 2 with +300 RSA analysis), and inexperienced (Obs. 3 with +50  
241 RSA analysis). For both static and dynamic radiographs, three of the previously analyzed radiographs (0°,  
242 30° and 60°) were used from each of the eight knees (n = 24). Each of the selected 24 static and 24

243 dynamic radiographs was reanalyzed two times (series 1 and series 2) with one week apart by all  
244 observers. The original image calibration and marker-model were kept intact in the radiographs, while the  
245 manual contour selection was redone, and therefore, the only possible difference in accuracy would be  
246 due to differences in the bone-models translation and rotation. After both analyses, the bone-models  
247 kinematic translation and rotation were extracted in all 6DOF.

## 248 **2.9 Data analysis:**

249 The raw kinematic data from the MBRSA-analysis were extracted and processed in customly developed  
250 software (MATLAB R2015b, Mathworks, USA).

251 For the following two statistical comparisons of the marker-method and the model-method, a mixed  
252 model was used, taking into account the repeated measurements on cadaver, pair, knee flexion angle,  
253 ligament combination and repetitions. Model validation was performed by visually inspecting the  
254 residuals and fitted values. Wald tests were used to analyze the systematic difference using a 0.05 level of  
255 significance.

256 1) To compare the bones individually, we calculated the error in translation and the rotation between the  
257 marker-method and the model-method using the Pythagorean Theorem;  $e = \sqrt{x^2 + y^2 + z^2}$ , with  $x$ ,  $y$   
258 and  $z$  being the error for either translations or rotations. Normally, the Pythagorean Theorem, cannot be  
259 used for rotations, but since the error in rotations is small, it is a good approximation (2). 2) The measured  
260 knee motion between the marker-method and the model-method was illustrated using Bland-Altman plots  
261 (20).

262 The mean error of rigid body fitting in femur and tibia was compared between static and dynamic  
263 radiographs using the Student's t-test.

264 For the intra-observer reliability measurements, the two image series from each observer were compared  
265 using Intra Class Correlation (ICC) and 95% confidence intervals. For the inter-observer reliability  
266 measurements, the three observers first analysis series ( $n = 24$ ) were compared using the ICC and 95%  
267 confidence intervals.

268

### 269 3. RESULTS

270 Figure d illustrates, for each leg, the error in translation and rotation between the model-method and the  
271 marker-method in both static and dynamic radiographs. The box to the far right marked “all” combines  
272 the errors of all legs, and Table 1, shows the statistical outcome of these combinations. The mean error in  
273 translation was maximal 0.62mm and for rotations maximal 0.96°. Femur had a significantly lower error  
274 compared to tibia in all examined groups except for translation in static radiographs. Comparing static and  
275 dynamic radiographs, the errors in the dynamic radiographs were only poorer for the tibia, while errors of  
276 the femur were not affected.

277 The mean differences between the model-method and marker-method of the 6DOF measured knee motion  
278 in the static and dynamic radiographs are shown in the Bland-Altman (BA) plots in Figure e. The BA plot  
279 for the static radiographs demonstrated a mean difference for all three rotations within  $-0.10 - 0.08^\circ$  and a  
280 Limit of Agreement (LoA) in the range  $\pm 0.76 - 1.26^\circ$ , while for the three translations, the mean was  
281 within  $-0.06 - 0.007\text{mm}$  LoA  $\pm 0.49 - 1.15\text{mm}$ . The dynamic radiographs showed a mean difference for the  
282 three rotations within  $-0.17 - 0.05^\circ$  LoA  $\pm 0.89 - 1.50$  and for the three translations the mean difference  
283 was within  $-0.23 - 0.16\text{mm}$  LoA  $\pm 0.75 - 1.34\text{mm}$ . The individual means and LoA's are presented in each  
284 subplot in Figure e. The differences in the means between the static and dynamic radiographs were small,  
285 while there was a tendency towards the dynamic radiographs having a larger LoA in all 6DOF. Visual  
286 inspections of the BA-plots for all 6DOF confirmed no concentration of observations and thereby no  
287 effect of either DOF or difference between intact and the knee with the ACL and ALL ligaments cut.

288 The roentgen systems post-processing software optimized continuously the image contrast of each  
289 radiograph during the dynamic sequences. Depending on the amount of the metal-fixture visible in the  
290 radiograph, the image contrast changed, making the bone-model less visible. The highest amount of metal  
291 was included in 60 degrees of knee flexion. With reduced clarity of the bone-model, the edge detection  
292 during analysis was harder due to some “washed out” bone edges. The contrast changed also in the static

293 radiographs, but due to the high quality of these radiographs, we did not experience difficulties with edge  
294 detection.

295 The average mean error in rigid body fitting of femur in static and dynamic radiographs were 0.046mm  
296 and 0.060mm ( $p=0.003$ ) respectively, and for the tibia in static 0.071mm and dynamic 0.080mm  
297 ( $p=0.116$ ).

298 The mean condition number and standard deviation for femur were 29.5 ( $\pm 19.1$ ) and for tibia 29.8  
299 ( $\pm 19.9$ ), indicating a good scatter of the markers.

300 The Intra-Class Correlation Coefficient (ICC [95% Confidence Interval]) for intra-observer reliability in  
301 the static radiographs were 0.98 [0.96;0.99] or better for all observers in all 6DOF. The ICC for inter-rater  
302 reliability for static radiographs were 0.99 [0.98;1.00] or better when comparing the kinematic results  
303 between all three observers in the 6DOF.

304 For the dynamic radiographs, the ICC for intra-observer reliability were 0.86 [0.68;0.94] or better for all  
305 observers. The ICC for inter-rater reliability among all observers were 0.95 [0.90;0.98] or better in the  
306 dynamic radiographs.

307 add a line in the results that a very experienced observer made a mistake of >5mm in 1 out of 24  
308 analyses performing the automated contour detection. “

309 The mean difference between the model-method and marker-method of the 6DOF measured knee motion  
310 in the static and dynamic radiographs were compared between all observers. In six of the 18 comparisons  
311 of static radiographs, a significant difference in the mean was found. No significant difference of the  
312 mean was found in the 18 comparisons in dynamic radiographs between observers.

#### 313 4.DISCUSSION

314 This study evaluated the accuracy of the CT model-method for measuring knee joint kinematics in static  
315 and dynamic RSA using the marker-method as the gold standard. As expected, the results generated with  
316 the model-method differed from the marker-method.

317 The mean difference between the model-method and the marker-method (systematic error) of all 6DOF in  
318 the kinematic analysis of the knee joint was found to be 0.23mm/° or better for both dynamic and static  
319 radiographs. The random error in terms of 95% LoA was largest in both static RSA  $\sim \pm 1.3^\circ$  and dynamic  
320 RSA  $\sim \pm 1.5^\circ$  in internal/external tibial rotation. This is to be expected since the model-method is  
321 generally less accurate for rotation about the long axis due to the cylindrical shape of long bones. The  
322 second and third largest LoA in dynamic RSA was found in medial-lateral translation and varus-valgus  
323 rotation, respectively. These directions were out-of-plane, which previously have been reported to have a  
324 worse accuracy compared to in-plane motion (10). For the static RSA, the out-of-plane medial-lateral  
325 translation had the second largest LoA as expected, while the in-plane anterior-posterior tibial translation  
326 had a slightly larger LoA compared to the out-of-plane varus-valgus rotation.

327 The LoA of the three in-plane DOF in static radiographs were  $\sim \pm 0.8\text{mm}$  or better, while for the dynamic  
328  $\sim \pm 1.1\text{mm}$  or better. The LoA was larger in all 6DOF when comparing the error of the dynamic to the  
329 static radiographs, which is similar to the results reported by Anderst et. al (7) when using biplane  
330 fluoroscopy and bone-models. Compared to that study (7), the present study found better or similar results  
331 for accuracy with dynamic RSA and bone-models, while for static RSA and bone-models our results were  
332 generally better for rotations, while generally worse for translations.

333 A comparison of the marker-method vs. model-method in dynamic and static radiographs (Table 1) for  
334 the two bones showed that the femur generally had a significantly lower mean total error compared to the  
335 tibia. This difference might be explained by the large size of the femoral condyles, opposite to the tibial  
336 plateau containing the eminencies, which are smaller bone parts and harder to locate on the radiographs.  
337 The result of the mean total difference between femur's marker-method and model-method did not differ  
338 when comparing dynamic and static radiographs as it did for tibia. A difference between static and  
339 dynamic radiographs was expected for both bones due to motion artifacts and the two times lower  
340 resolution in the dynamic radiographs.

341 For both the static and dynamic radiographs, the mean rigid body errors were within the limit of 0.35mm  
342 that are normally used in RSA analysis. The mean error of the markers was significantly higher for femur  
343 in the dynamic radiographs compared to the static radiographs, while it was not for tibia. This difference  
344 can have two causes: First; the lower resolution of the dynamic radiographs results in less accurate marker  
345 projection detection. Second; the motion artifacts of the bone moving in the dynamic radiographs results  
346 in less accurate marker projection detection. We expect the lower resolution having the largest influence  
347 as the leg moved very slow compared to the 2.5ms pulse width and the roentgen tubes were synchronized  
348 within 0.002ms with a maximum allowed time delay of 0.1ms.

349 A probable cause for the observed difference in error for the tibia between static and dynamic radiographs  
350 could be the anatomical shape of tibia's bone. The pose estimation of the tibia might have been worse,  
351 due to less good software recognition of especially the tibial plateau and eminencies when detecting edge  
352 contours. Further, the model-method was sensitive to image contrast changes, which inevitably occurred  
353 when the metal-fixture moved into the image during knee flexion. This automatic contrast adjustment of  
354 the roentgen system might also have had a negative effect on the visibility of thin bone parts of the tibial  
355 plateau as compared to the thicker cortical bone of the femoral condyles.

356 The Bland-Altman plots confirmed no concentration of observations, which was possible, since the clarity  
357 of the bone-model was reduced with the metal-fixture gradually moving into the image. Thus, the  
358 difference between the model-method and the marker-method could have been largest at 60°.

359 Additionally, no concentration were found between the intact- and the knees with ACL and ALL ligament  
360 removed, confirming the model-method to be reliable in measurements of the knee joint with different  
361 ligament situations.

362 Both the intra- and inter-observer reliability measurements for the manual contour detection in static and  
363 dynamic radiographs were very good. These results are similar to the results found in a study using  
364 ModelBasedRSA to detect hip arthroplastic wear, where both the correlation in intra- and inter-observer  
365 reliability measurements were 0.997 or better in all cases (21).

366 However, in the present study, observer 2's calculated ICC for medial-lateral tibial translation in the  
367 dynamic radiographs was particular worse than the rest of the calculated ICC's, and was 0.86 [0.68 ;0.94].  
368 The lower ICC score was caused by a mistake during analysis of one radiograph, which resulted in a  
369 translation error of -5.43 mm between tibias bone-model and marker-model. We did not reanalyze the  
370 radiograph, but it was detected as an outlier during the kinematic calculations, and could normally have  
371 been reanalyzed. By removing this single erroneous radiograph from the ICC calculation, the ICC  
372 increased from 0.86 [0.68 ;0.94] to 0.98 [0.95 ;0.99].

373 High correlations were expected in the present study, as the bone contours are detected automatically by  
374 the software and only have to be selected by the observer. As the contours are clickable, the "correct"  
375 contours are fairly easy to select, and we would expect lower correlations, if the observers were to draw  
376 the bone contours themselves instead of selecting them.

377 The mean kinematic difference between the marker-method and the model-method were calculated for  
378 the first series of analysis of each observer. These differences were calculated to investigate if one  
379 observer were significantly more accurate compared to the others. No observer was found to be better  
380 than the others regardless of their different experience level with model-based RSA.

381 It is not easy to compare our results to previously reported results. Most studies have either used biplane  
382 fluoroscopy and bone-models (7,22,23), RSA combined with models of metal prosthesis (10,24), or bone  
383 models (25), while to our knowledge, no accuracy studies have been reported using dynamic RSA and  
384 bone-models. Models of metal prosthesis have clear edges for contrast detection, while bones differ due  
385 to bone quality and comparisons between these methods are therefore not just. The accuracy results of the  
386 study by Seehaus (25) are worse than the results presented in the current study, which is most likely  
387 caused by cutting away the proximal tibia and distal femur for the placement of a knee prosthesis.

388 Knowledge of the accuracy and limitations of both the marker-method and the model-method will help us  
389 in the choice of the more appropriate method in future studies. The marker-method is still the gold

390 standard method (markers = submillimeter precision), but the advantage of the model-method is that pre-  
391 operatively measurements are also possible without implanted markers. Further, the bone-model offers a  
392 good non-invasive and alternative method for measurements of in-vivo knee kinematics, and no other  
393 similarly precise methods or tools are available. However, even though no implanted markers are needed,  
394 it is important to consider the additional required CT radiation dose with respect to the added benefit of a  
395 study before including patients. Further, researchers should be encouraged to perform relatively short  
396 dynamic experiments with live tissue involved.

397 In the future, we believe, the bone-model-method could be used for in-vivo studies of knee joint  
398 kinematics performed at a slow pace, and could potentially be developed further for clinical use as a  
399 diagnostic tool for assessment of ligament laxity. However, for the method to be truly effective an  
400 automated image analysis system with minimal necessary human interaction is required, since the time  
401 spend on manual analysis is prohibitive. In summary, this study found the mean error of CT bone-models  
402 combined with static RSA to be  $\sim -0.001^\circ$  with a maximum limit of agreement (LoA) in rotations of  
403  $\pm 1.26^\circ$  or better, while for translations it was  $\sim -0.03\text{mm}$  LoA  $\pm 1.15\text{mm}$  or better. For the dynamic  
404 radiographs, the mean error for rotations was  $\sim -0.11^\circ \pm 1.50^\circ$  or better and  $\sim -0.04\text{mm}$  LoA  $\pm 1.34\text{mm}$  or  
405 better for translations. These results may encourage the use of bone-models and dynamic RSA for non-  
406 invasive kinematic knee joint analysis in the future. In conclusion, the CT model method combined with  
407 dynamic RSA may be an alternative to prior marker-based methods for kinematic analyses in a laboratory  
408 controlled setting.

409

## 410 5. REFERENCES

- 411 1. Benoit DL, Ramsey DK, Lamontagne M, Xu L, Wretenberg P, Renström P. Effect of skin  
412 movement artifact on knee kinematics during gait and cutting motions measured in vivo. *Gait*  
413 *Posture*. 2006 Oct;24(2):152–64.
- 414 2. Selvik G. Roentgen stereophotogrammetry. A method for the study of the kinematics of the  
415 skeletal system. *Acta Orthop Scand Suppl*. 1989 Jan;232:1–51.

- 416 3. Van Embden D, Stollenwerck G a. NL, Koster L a., Kaptein BL, Nelissen RGHH, Schipper IB.  
417 The stability of fixation of proximal femoral fractures: a radiostereometric analysis. *Bone Joint J.*  
418 2015;97-B(3):391–7.
- 419 4. Molt M, Toksvig-Larsen S. 2-Year Follow-Up Report on Micromotion of a Short Tibia Stem. *Acta*  
420 *Orthop.* 2015;86(5):594–8.
- 421 5. Kärrholm J. Roentgen stereophotogrammetry. Review of orthopedic applications. *Acta Orthop*  
422 *Scand.* 1989 Mar 30;60(4):491–503.
- 423 6. Bojan AJ, Bragdon C, Jönsson A, Ekholm C, Kärrholm J. Three-dimensional bone-implant  
424 movements in trochanteric hip fractures: Precision and accuracy of radiostereometric analysis in a  
425 phantom model. *J Orthop Res.* 2015;n/a – n/a.
- 426 7. Anderst W, Zauel R, Bishop J, Demps E, Tashman S. Validation of three-dimensional model-  
427 based tibio-femoral tracking during running. *Med Eng Phys.* 2009;31(1):10–6.
- 428 8. Tashman S, Anderst W. In-vivo measurement of dynamic joint motion using high speed biplane  
429 radiography and CT: application to canine ACL deficiency. *J Biomech Eng.* 2003;125(2):238–45.
- 430 9. Anderst WJ, Baillargeon E, Donaldson WF, Lee JY, Kang JD. Validation of a noninvasive  
431 technique to precisely measure in vivo three-dimensional cervical spine movement. *Spine (Phila*  
432 *Pa 1976).* 2011;36(6):E393–400.
- 433 10. Kaptein BL, Valstar ER, Stoel BC, Rozing PM, Reiber JHC. A new model-based RSA method  
434 validated using CAD models and models from reversed engineering. *J Biomech.* Elsevier; Jun  
435 1;36(6):873–82.
- 436 11. Valstar ER, De Jong FW, Vrooman H a., Rozing PM, Reiber JHC. Model-based Roentgen  
437 stereophotogrammetry of orthopaedic implants. *J Biomech.* Elsevier; 2001 Apr 30;34(6):715–22.
- 438 12. Stagni R, Fantozzi S, Cappello A, Leardini A. Quantification of soft tissue artefact in motion  
439 analysis by combining 3D fluoroscopy and stereophotogrammetry: a study on two subjects. *Clin*  
440 *Biomech.* 2005;20(3):320–9.
- 441 13. Garling EH, Kaptein BL, Mertens B, Barendregt W, Veeger HEJ, Nelissen RGHH, et al. Soft-  
442 tissue artefact assessment during step-up using fluoroscopy and skin-mounted markers (*Journal of*  
443 *Biomechanics* (2007) 40, SUPPL. 1, (S18-S24) DOI: 10.1016/j.jbiomech.2007.03.003). *J*  
444 *Biomech.* 2008;41(10):2332–3.
- 445 14. Krčah M, Székely G, Blanc R. Fully automatic and fast segmentation of the femur bone from 3D-  
446 CT images with no shape prior. *Proc - Int Symp Biomed Imaging.* 2011;2087–90.
- 447 15. De Raedt S, Mechlenburg I, Stilling M, Rømer L, Søballe K, de Bruijne M. Automated  
448 measurement of diagnostic angles for hip dysplasia. *SPIE Med Imaging, Int Soc Opt Photonics.*  
449 2013;867009–867009.
- 450 16. Boykov Y, Funka-Lea G. Graph cuts and efficient N-D image segmentation. *Int J Comput Vis.*  
451 2006;70(2):109–31.

- 452 17. Kaptein BL, Valstar ER, Stoel BC, Rozing PM, Reiber JHC. Evaluation of three pose estimation  
453 algorithms for model-based roentgen stereophotogrammetric analysis. Proc Inst Mech Eng H.  
454 2004;218(4):231–8.
- 455 18. Valstar ER, Gill R, Ryd L, Flivik G, Börlin N, Kärrholm J. Guidelines for standardization of  
456 radiostereometry (RSA) of implants. Acta Orthop. 2005;76(4):563–72.
- 457 19. Iso16087. ISO 16087:2013 Implants for surgery — Roentgen stereophotogrammetric analysis for  
458 the assessment of migration of orthopaedic implants. 2013;2013.
- 459 20. Bland JM, Altman DG. Measuring agreement in method comparison studies. Stat Methods Med  
460 Res. 1999;8(2):135–60.
- 461 21. Pineau V, Lebel B, Gouzy S, Dutheil JJ, Vielpeau C. Dual mobility hip arthroplasty wear  
462 measurement: Experimental accuracy assessment using radiostereometric analysis (RSA). Orthop  
463 Traumatol Surg Res. 2010;96(6):609–15.
- 464 22. Li G, Van de Velde SK, Bingham JT. Validation of a non-invasive fluoroscopic imaging technique  
465 for the measurement of dynamic knee joint motion. J Biomech. 2008 Jan;41(7):1616–22.
- 466 23. Tashman S, Bey MJ, Anderst W, Demps E, Zauel R. MODEL-BASED TRACKING OF KNEE  
467 KINEMATICS FROM BIPLANE RADIOGRAPHS: IN-VIVO VALIDATION. 52nd Annu Meet  
468 Orthop Res Soc. (Paper No: 0252).
- 469 24. Hurschler C, Seehaus F, Emmerich J, Kaptein BL, Windhagen H. Comparison of the Model-Based  
470 and Marker-Based Roentgen Stereophotogrammetry Methods in a Typical Clinical Setting. J  
471 Arthroplasty. Elsevier Inc.; 2009 Jun 1;24(4):594–606.
- 472 25. Seehaus F, Olender GD, Kaptein BL, Ostermeier S, Hurschler C. Markerless Roentgen  
473 Stereophotogrammetric Analysis for in vivo implant migration measurement using three  
474 dimensional surface models to represent bone. J Biomech. Elsevier; 2012;45(8):1540–5.

475

476

## 477 **6.FIGURES AND TABLES:**

478 Figure a – CT bone-model of the femur to the left and the tibia to the right with their local coordinate  
479 systems.

480 Figure b – Simple drawing of the setup.

481 Figure c – Left: Static radiographic image. Right: Dynamic radiographic image. The zoomed images  
482 show the resolution in the static image being two times higher compared to the dynamic image. The  
483 yellow and green circles indicate the fiducial and control markers in the calibration box. The dynamic  
484 radiograph is inverted compared to the static radiograph and is a standard setting of the RSA system,  
485 which was not changed prior to the recordings, however this difference poses no issues in analysis of the  
486 radiographs.

487 Figure d – The upper boxplot show the combined three-axis translation error and three-axis rotation error  
488 between the model-method and the marker-method in the static radiographs, whereas the lower boxplots  
489 illustrates the dynamic radiographs. Each box display the median, the 25th and 75th percentiles, while  
490 the whiskers extend to the most extreme points not considered outliers. Circles are outliers  $> \pm 2.7$  SD.  
491 Each bar (A-H) is a donor leg and the bar marked “all” is data from all the cadavers combined. A-B, C-D,  
492 E-F and G-H are paired legs from the same subject.

493 Figure e – The upper Bland-Altman plot show the CT bone-model compared to the marker-method of the  
494 static radiographs in all 6DOF, while the lower BA plot show data from the dynamic radiographs. Circles  
495 = 0°, Crosses = 30°, Squares = 60°. Blue observations = intact knee. Pink observations = with both the  
496 ACL and ALL ligaments cut. The p-value indicates if the mean is significant different from zero.

497 Table 1 – Mean error of the boxes marked “all” from figure 4. The p-value indicates the comparison of  
498 static and dynamic radiographs in the upper part of the table, while the total error of femur and tibia are  
499 compared in the lower part of the table.

500

## 501 **ACKNOWLEDGEMENTS**

502 We thank the department of Radiology at Aarhus University Hospital for their support, and especially  
503 Lars Lindgren and Mark Jensen for their help with recording the radiographs. Further we thank the  
504 Department of Biomedicine at Aarhus University for providing the donor specimens. Also, we would like  
505 to thank Smith and Nephew Denmark for making the instruments for surgery and the arthroscopic  
506 hardware available. This work was supported by six funds; 1) Innovation Fund Grant 69-2013-1  
507 “Transforming radiological technology for assessment of implant fixation: from research tool to clinical  
508 application”, 2) Civilingeniør Frode V. Nyegaard og Hustrus fond, 3) Ortopædkirurgisk forskningsfond i  
509 Aarhus, 4) A.P Møller Fonden – Fonden til Lægevidenskabens fremme, 5) Grosserer L. F. Foghts Fond,  
510 6) Helga og Peter Kornings Fond. These six funds had no influence on the study design or the results.

511

512

513

514

515

516

517

518

519

## **Conflict of Interest Statement**

520

521

522

523

524

525 The authors of this paper have no financial or personal relationships with other people or organizations  
526 that could inappropriately influence (bias) our work, but it should be noted that Sepp De Raedt was  
527 employed at Nordisk Røntgen Teknik as a software developer during the study, and Bart L. Kaptein has  
528 been a part of the developing team of the software Model Based RSA.

529

530

531

532

533

534

535

Kasper Stentz-Olesen

536

Emil Toft Nielsen

537

Sepp De Raedt

538

Peter Bo Jørgensen

539

Ole Gade Sørensen

540

Bart L. Kaptein

541

Michael S. Andersen

542

Maiken Stilling

543

544

Figure a

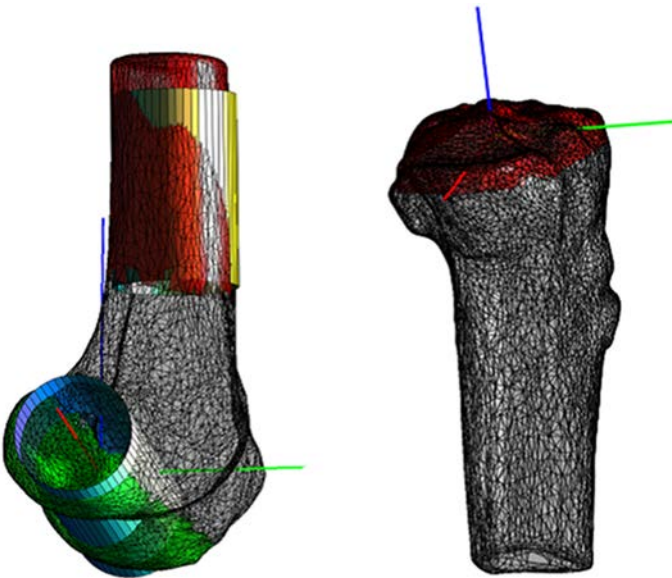


Figure b

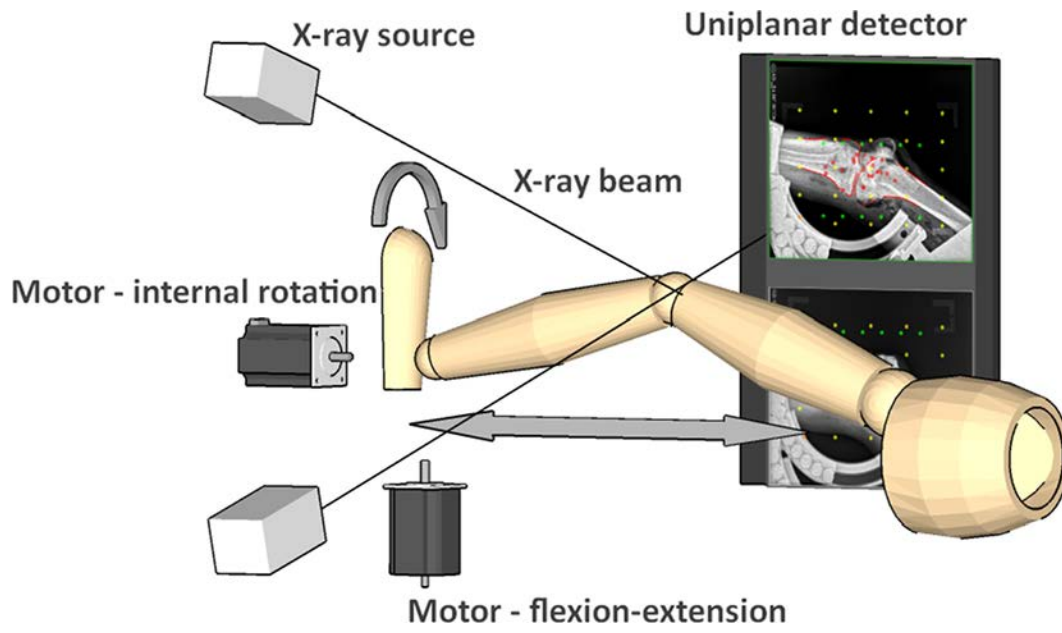


Figure c

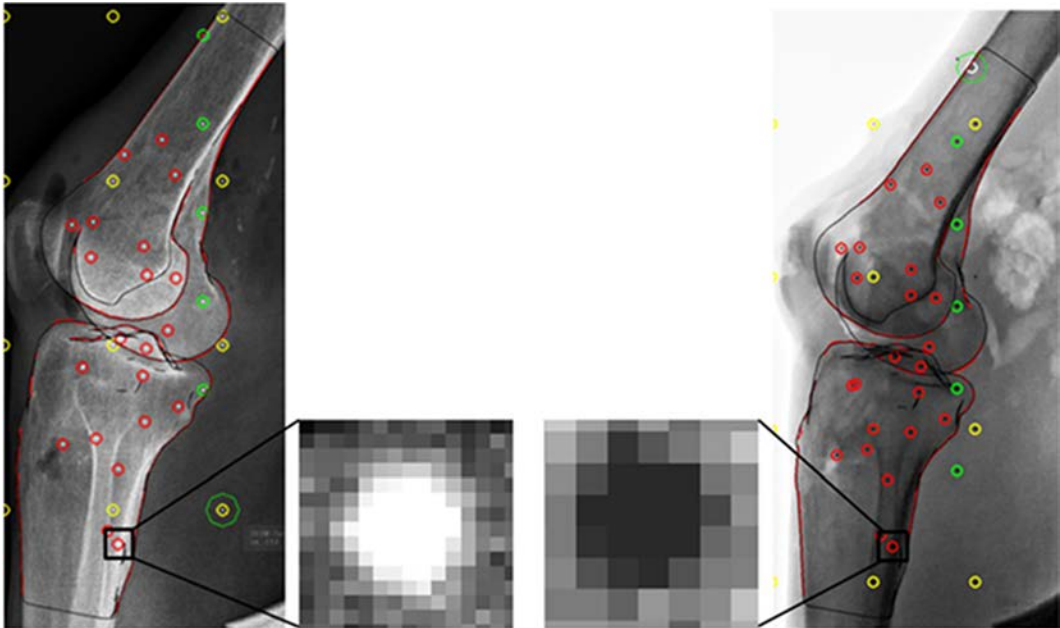


Figure d

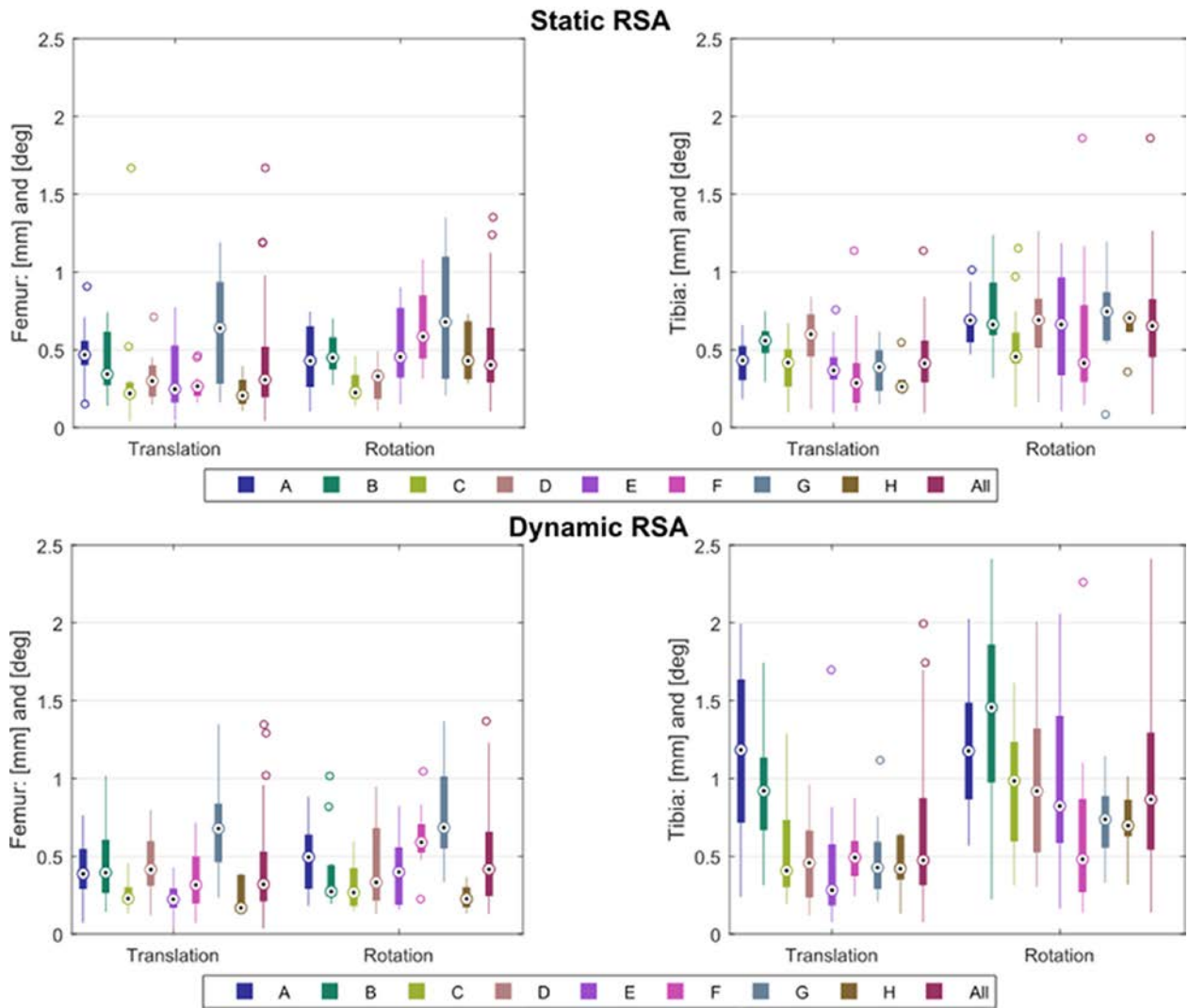
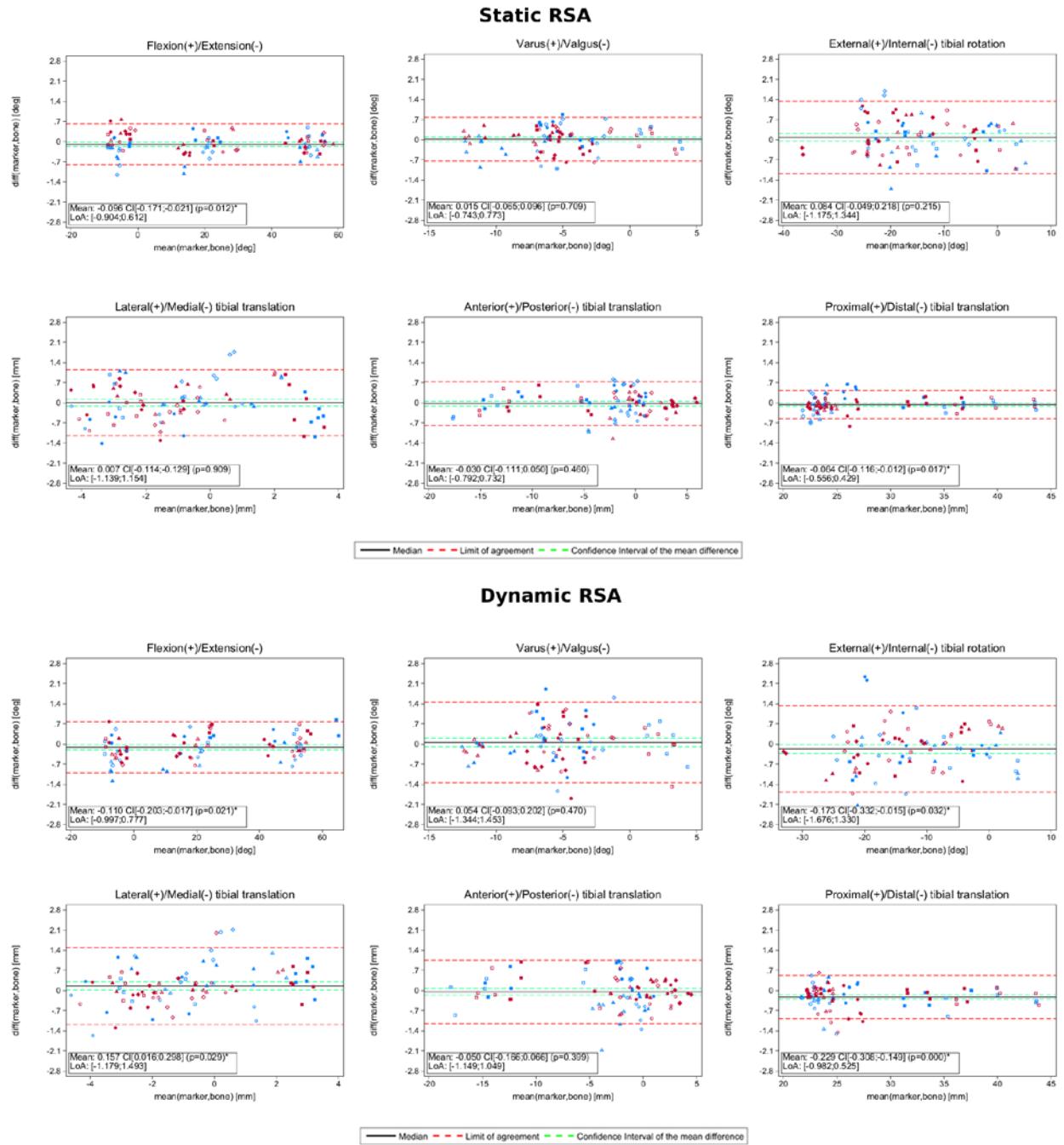


Figure e



**Tabel 1**

n = 89	Mean	CI	Mean	CI	P-value
	Static		Dynamic		
Femur – Translation [mm]	0.384	[0.284 ; 0.484]	0.391	[0.296 ; 0.487]	0.833
Femur – Rotation [deg]	0.477	[0.349 ; 0.605]	0.479	[0.389 ; 0.610]	0.948
Tibia – Translation [mm]	0.425	[0.344 ; 0.506]	0.619	[0.506 ; 0.733]	0.000
Tibia – Rotation [deg]	0.659	[0.571 ; 0.746]	0.960	[0.840 ; 1.081]	0.000
	Femur		Tibia		
Static – Translation [mm]	0.387	[0.317 ; 0.457]	0.429	[0.375 ; 0.482]	0.190
Static – Rotation [deg]	0.483	[0.358 ; 0.608]	0.665	[0.531 ; 0.799]	0.000
Dynamic – Translation [mm]	0.391	[0.291 ; 0.490]	0.620	[0.496 ; 0.743]	0.000
Dynamic – Rotation [deg]	0.469	[0.381 ; 0.557]	0.955	[0.823 ; 1.087]	0.000